Thermosolutal Natural Convection in Horizontal Elliptical Annulus Containing a Fluid-saturated Porous Medium: Effects of Aiding Buoyancy for Low Rayleigh-Darcy Number

Hichem Boulechfar, *Member IAENG*, Mahfoud Djezzar

***Abstract*—Two-dimensional thermosolutal natural convection in an annular elliptical space filled with a fluid-saturated porous medium, is analyzed by solving numerically the mass balance, momentum, energy and concentration equations, using Darcy's law and Boussinesq approximation. Two walls delimiting the annular space are maintained at two uniform different temperatures and concentrations. The external parameters considered are the Rayleigh-Darcy number and the buoyancy ratio. There are two main approaches of thermosolutal natural convection; the aiding and opposing buoyancies. For the present work, the heat and mass transfer natural convection is studied for the case of aiding buoyancy effects, where the flow is generated by both temperature and solutal concentration gradients. The Average Nusselt and Sherwood numbers are presented in terms of the external parameters mentioned above.**

***Index Terms*— Thermosolutal, Natural convection, Porous media, Elliptical annulus, buoyancy effects**

I. Introduction

During recent years, innumerable theoretical, numerical and experimental studies have dealt with heat and mass transfer confined into different vertical and horizontal annular enclosures; these annular spaces have different geometries and can be partly or completely filled with a porous media. The most research effort has been devoted to the study of heat and mass transfer induced in a porous medium saturated by a fluid for non-curved geometries the horizontal cylindrical and elliptical annulus geometries were particularly subject of a considerable studies but for the case of heat transfer. Interest in the phenomena of heat and mass transfer by natural convection is due to many potential applications in the engineering processes.

Manuscript received March 29, 2014; revised April 3, 2014

Hichem Boulechfar is with the Physics and Energy Laboratory, Faculty of Exact Sciences, University of Constantine 1, Aïn El Bey Street, 25000 Constantine, Algeria

E-mail:boulechfar_hichem@yahoo.fr

Mahfoud Djezzar is with the Physics and Energy Laboratory, Faculty of Exact Sciences, University of Constantine 1, Aïn El Bey Street, 25000 Constantine Algeria

E-mail:mdjezzar@umc.edu.dz

The applications involve the chemical industry, reservoir engineering in connection with thermal recovery process and the study of dynamics of hot and salty springs of a sea, the underground spreading of chemical waste and other pollutants. The security issues in the heart of nuclear reactors, evaporation cooling and solidification are few other application areas where combined thermo-solutal convection in porous media can be observed. Sankar and al. [1] investigated natural convection flows in a vertical annulus filled with a fluid-saturated porous medium, when the inner wall is subject to discrete heating. The outer wall is maintained isothermally at a lower temperature, while the top and bottom walls, and the unheated portions of the inner wall are kept adiabatic. Through the Brinkman-extended Darcy equation, the relative importance of discrete heating on natural convection in the porous annulus is examined. An implicit finite difference method has been used to solve the governing equations of the flow system. The analysis is carried out for a wide range of modified Rayleigh and Darcy numbers for different heat source lengths and locations.

F.M. Mahfouz [2] has investigated a buoyancy driven flow and associated heat convection in an elliptical enclosure. The enclosure which is the space between two horizontal concentric confocal elliptic tubes is heated through its inner tube surface which is maintained at either uniform temperature or uniform heat flux. The induced buoyancy driven flow and the associated heat convection are predicted at different enclosure orientations. The full governing equations in terms of vorticity, stream function and temperature are solved numerically using Fourier Spectral Method. Khanafer and al. [3] studied a numerical investigation of natural convection heat transfer within a two-dimensional, horizontal annulus that is partially filled with a fluid-saturated porous medium. In addition, the porous sleeve is considered to be press fitted to the inner surface of the outer cylinder. Both cylinders are maintained at constant and uniform temperatures with the inner cylinder being subjected to a relatively higher temperature than the outer one. Moreover, the Forchheimer and Brinkman effects are taken into consideration when simulating the fluid motion inside the porous sleeve. Kumari and Nath [4] studied the unsteady natural convection flow from a horizontal cylindrical annulus filled with a non-Darcy porous medium .The unsteadiness in the problem arises due

ISBN: 978-988-19253-5-0
ISSN: 2078-0958 (Print); ISSN: 2078-0966 (Online)

to the impulsive change in the wall temperature of the outer cylinder. The Navier–Stokes equations along with the energy equation governing the unsteady natural convection flow have been solved by the finite-volume method. The results show that the annulus completely filled with a porous medium has the best insulating effectiveness. The effect of Darcy number on the heat transfer is more pronounced than that of the Grashof number. Yong Shi and al. [5]presented a finite difference-based lattice BGK model for thermal flows is proposed based on the double-distribution function approach; they applied this model to simulate natural convection heat transfer in a horizontal concentric annulus bounded by two stationary cylinders with different temperatures. Velocity and temperature distributions as well as Nusselt numbers were obtained for the Rayleigh numbers ranging from $2.38x10^3$ to $1.02x10^5$ with the Prandtl number around 0.718. Edimilson J and al. [6] examined a numerical computation for laminar and turbulent natural convection within a horizontal cylindrical annulus filled with a fluid saturated porous medium. Computations covered the range of $25 < Ra_m < 500$ and $3.2x10^{-4} > Da > 3.2x10^{-6}$ and made use of the finite volume method. The inner and outer walls are maintained at constant but different temperatures. The macroscopic k–e turbulence model with wall function is used to handle turbulent flows in porous media.

Leong and Lai [7] presented a natural convection in concentric cylinders with a porous sleeve, analytical solutions obtained through perturbation method and Fourier transform. The porous sleeve is press-fitted to the inner surface of the outer cylinder. Both the inner and outer cylinders are kept at constant temperatures with the inner surface at a slightly higher temperature than that of the outer. The main objective of this study is to investigate the buoyancy-induced flow as affected by the presence of the porous layer. A parametric study was performed to investigate the effects of Rayleigh number, Darcy number, porous sleeve thickness, and relative thermal conductivity on the heat transfer results. M. Djezzar and al. [8] expressed the Boussinesq equations of the laminar thermal and natural convection, in the case of permanent and bidimensional flow, in an annular space between two confocal elliptic cylinders using a new calculation code of the finite volumes with the primitive functions (velocity-pressure formulation) in the elliptic coordinates system. Both effects of Rayleigh number and the geometry of the interior elliptic cylinder were examined. Y.D. Zhu and al. [9] presented a natural convective heat transfer between two horizontal, elliptic cylinders that was numerically studied using the differential quadrature (DQ) method. The governing equations are taken to be in the vorticity-stream function formulation. The coordinate transformation was performed to apply the DQ method. An elliptic function was used, which makes the coordinate transformation from the physical domain to the computational domain be set up by an analytical expression. The present method was validated by comparing its numerical results with available publication data and very good agreement has been achieved. A systematic study is conducted for the analysis of flow and thermal fields at different eccentricities and angular positions.

Wassim C. and al. [10] presented a new calculation code using a two-dimensional finite element method valid in a steady and laminar flow within an annular enclosure which is represented by inner circular and outer elliptical cylinders. The Rayleigh number is large enough; there exists an interval of values of Rayleigh number for which the relaxation coefficients do not only influence the speed of calculation convergence but also the solution of transfer equation.

Mota and al. [11] solved the two-dimensional Darcy-Boussinesq equations, governing natural convection heat transfer in a saturated porous medium, in generalized orthogonal coordinates, using high-order compact finites differences on a very fine grid. The mesh is generated numerically using the orthogonal trajectory method. The code is applied to horizontal eccentric elliptic annuli containing saturated porous media. The judicious stretching of one of the annular walls in the horizontal direction reduces the heat losses with respect to a concentric cylindrical annulus with the same amount of insulating material. Charrier-Mojtabi [12] carried a numerical investigation of two-dimensional and three-dimensional free convection flows in a saturated porous horizontal annulus heated from the inner surface, using a Fourier-Galerkin approximation for the periodic azimuthal and axial directions and a collocation-Chebyshev approximation in the confined radial direction. The numerical algorithm integrates the Darcy-Boussinesq's equations formulated in terms of pressure and temperature. This method gives an accurate description of the 2-D multicellular structures for a large range of Rayleigh number and radii ratio.

M. M. Elshamy and M. N. Ozisik [13] studied numerically a steady-state natural convection for air bounded by two confocal horizontal elliptical cylinders for the case of inner hot and outer cold isothermal surfaces. The local and average Nusselt numbers were determined for different value of Rayleigh number for different eccentricities of the inner surface.

II. NOMENCLATURE

Symbol	Definition	Unit
a	Thermal diffusivity	m^2/s
A	Elliptic cylinder major axis	m
B	Elliptic cylinder minor axis	m
c	Constant defined in elliptic coordinates	m
c_p	Specific heat at constant pressure	$J/kg.K$
D	Concentration diffusivity	m^2/s
C	Mass concentration	g/l
C_1	Inner wall's concentration	g/l
C_2	Outer wall's concentration	g/l
Da	Darcy number	
e	Elliptic cylinder eccentricity, $\left[=\sqrt{\frac{(A^2-B^2)}{A^2}}\right]$	
g	Gravitational acceleration	m/s^2
Gr	Grashof number, $[=g\beta c^3(T_1-T_2)/\upsilon^{-2}]$	
h	Dimensional metric coefficient	m
H	Dimensionless metric coefficient	
K	Porous medium permeability	m^2
Le	Lewis Number	
N	Buoyancy ratio, $[=\beta c\Delta C/\beta_T\Delta T]$	
Nu	Local Nusselt number	

ISBN: 978-988-19253-5-0
ISSN: 2078-0958 (Print); ISSN: 2078-0966 (Online)

P	Pressure	N/m^2
Pr	Prandtl number	
Ra	Rayleigh number, [=$Gr.Pr$]	
Ra_m	Rayleigh-Darcy number, [=$Ra.Da$]	
Sh	Local Sherwood number	
t	Time	s
T	Fluid's temperature	K
T_1	Inner wall's temperature	K
T_2	Outer wall's temperature	K
u	Velocity component-coordinate x	m/s
v	Velocity component-coordinate y	m/s
U_η	Velocity component-coordinate η	m/s
V_θ	Velocity component-coordinate θ	
$\vec{V}$	Velocity vector	m/s
x, y	Cartesian coordinates	m

Greek Letters

α	Inclination angle	◦
β_C	Concentration expansion coefficient	$(g/l)^{-1}$
β_T	Thermal expansion coefficient	K^{-1}
λ	Thermal conductivity	$W/m.K$
υ	Kinematic viscosity,	m^2/s
ε	Porosity	
σ_T	Thermal capacity factor	
ΔC	Concentration difference, [=C_1-C_2]	g/l
ΔT	Temperature difference, [=T_1-T_2],	K
ρ	Density	kg/m^3
ψ	Stream function	m^2/s
η, θ	Elliptic coordinates	

Subscripts

1	Inner
2	Outer
p	Porous

Superscripts

+	Dimensionless parameters

III. Problem Formulation And Basic Equation

We consider a thermosolutal natural convection in an annular elliptical space filled with fluid-saturated porous medium; Fig. 1 represents a cross section of the system. Both elliptic internal and external walls are isothermal and impermeable, kept at constant temperatures and concentrations *T1, C1* and *T2, C2* respectively with *T1>T2* and *C1>C2*. The physical properties of the fluid are constant, apart from the density ρ whose variations are at the origin of the natural convection.

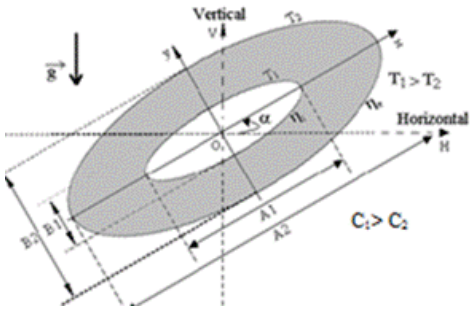

Fig. 1. The cross section of the system

Viscous dissipation is neglected, just as the radiation (emissive properties of the two walls being neglected). Soret and Dufour effects are neglected and we admit that the problem is bidimensional, permanent and laminar. The porous medium is considered isotropic and homogeneous. The heat and mass transfer by natural convection is represented by the following equations within the framework of the Boussinesq approximation:

A. Continuity Equation

$$div\vec{V} = 0 \tag{1}$$

B. Momentum Equation

The classic formulation of Darcy is used for writing the equation of motion:

$$\vec{V} = \frac{K}{\mu}\left(-\nabla P + \rho\vec{g}\right) \tag{2}$$

C. Heath Equation

$$\sigma_T \frac{\partial T}{\partial t} + \left(\vec{V}\cdot\overrightarrow{\text{grad}}\right)T = \frac{\lambda_p}{\rho C_p}\nabla^2 T \tag{3}$$

D. Concentration Equation

$$\varepsilon\frac{\partial C}{\partial t} + \left(\vec{V}\cdot\overrightarrow{\text{grad}}\right)C = D\nabla^2 C \tag{4}$$

The Boussinesq approximation for the combined heat and mass transfer is written as following:

$$\rho = \rho_0\left(1-\beta_T\left(T-T_0\right)-\beta_C\left(C-C_0\right)\right) \tag{5}$$

It is convenient to define a reference frame such as the limits of the system result in constant values of the coordinates. The passage from the Cartesian coordinates (x, y) to the elliptic coordinates (η,θ) is obtained by the following relations:

$$\left.\begin{aligned} x &= c.ch(\eta).\cos(\theta) \\ y &= c.sh(\eta).\sin(\theta) \end{aligned}\right\} \tag{6}$$

Equations (1), (2),(3) and (4) are written respectively:

$$\frac{\partial}{\partial\eta}\left(hV_\eta\right)+\frac{\partial}{\partial\theta}\left(hV_\theta\right)=0 \tag{7}$$

$$\frac{1}{h}\left[\frac{\partial^2\psi}{\partial\eta^2}+\frac{\partial^2\psi}{\partial\theta^2}\right]=-\frac{Kg\beta}{\upsilon}\left(\left[\cos(\alpha)F(\eta,\theta)-\sin(\alpha)G(\eta,\theta)\right]\left(\frac{\partial T}{\partial\eta}+N\frac{\partial C}{\partial\eta}\right)-\left[\sin(\alpha)F(\eta,\theta)+\cos(\alpha)G(\eta,\theta)\right]\left(\frac{\partial T}{\partial\theta}+N\frac{\partial C}{\partial\theta}\right)\right) \tag{8}$$

$$V_\eta\frac{\partial T}{\partial\eta}+V_\theta\frac{\partial T}{\partial\theta}=a\left(\frac{1}{h^2}\right)\left[\frac{\partial^2 T}{\partial\eta^2}+\frac{\partial^2 T}{\partial\theta^2}\right] \tag{9}$$

$$V_\eta\frac{\partial C}{\partial\eta}+V_\theta\frac{\partial C}{\partial\theta}=D\left(\frac{1}{h^2}\right)\left[\frac{\partial^2 C}{\partial\eta^2}+\frac{\partial^2 C}{\partial\theta^2}\right] \tag{10}$$

ISBN: 978-988-19253-5-0
ISSN: 2078-0958 (Print); ISSN: 2078-0966 (Online)

Vη and Vθ are the velocity components in the directions η and θ. Metric coefficients in elliptic coordinates are given by: $h = h_1 = h_2 = c\left(sh^2(\eta) + sin^2(\theta)\right)^{1/2}$, $h_3 = 1$

with $c = \frac{A}{ch(\eta)} = \frac{B}{sh(\eta)}$

$$F(\eta,\theta) = \frac{sh(\eta)cos(\theta)}{\left(sh^2(\eta)+sin^2(\theta)\right)^{1/2}} \quad , \quad G(\eta,\theta) = \frac{ch(\eta)sin(\theta)}{\left(sh^2(\eta)+sin^2(\theta)\right)^{1/2}}$$

The characteristic quantities used for the dimensionless problem between the inner and the outer elliptic cylinder are the characteristic temperature and concentration $\Delta T = T1 - T2$, $\Delta C = C1 - C2$. The focal length c in the elliptic coordinates is the reference length and the thermal diffusivity of the fluid a, the ratio of the thermal diffusivity and the characteristic length *c (a/c)* is the characteristic velocity. The dimensionless mathematical model obtained is expressed by the following equations:

$$\frac{\partial}{\partial\eta}\left(HV_\eta^+\right) + \frac{\partial}{\partial\theta}\left(HV_\theta^+\right) = 0 \tag{11}$$

$$HV_\eta^+\frac{\partial T^+}{\partial\eta} + HV_\theta^+\frac{\partial T^+}{\partial\theta} = \left[\frac{\partial^2 T^+}{\partial\eta^2} + \frac{\partial^2 T^+}{\partial\theta^2}\right] \tag{12}$$

$$HV_\eta^+\frac{\partial C^+}{\partial\eta} + HV_\theta^+\frac{\partial C^+}{\partial\theta} = \frac{1}{Le}\left[\frac{\partial^2 C^+}{\partial\eta^2} + \frac{\partial^2 C^+}{\partial\theta^2}\right] \tag{13}$$

$$\frac{1}{h}\left[\frac{\partial^2\psi^+}{\partial\eta^2} + \frac{\partial^2\psi^+}{\partial\theta^2}\right] = -Ra_m.H\left(\left[\cos(\alpha)F(\eta,\theta) - \sin(\alpha)G(\eta,\theta)\right]\left(\frac{\partial T^+}{\partial\eta} + N\frac{\partial C^+}{\partial\eta}\right) - \left[\sin(\alpha)F(\eta,\theta) + \cos(\alpha)G(\eta,\theta)\right]\left(\frac{\partial T^+}{\partial\theta} + N\frac{\partial C^+}{\partial\theta}\right)\right) \tag{14}$$

Where Vη, Vθ are the components of the dimensionless velocity defined by:

$$V_\eta^+ = \frac{1}{H}\frac{\partial\psi^+}{\partial\theta},\ V_\theta^+ = -\frac{1}{H}\frac{\partial\psi^+}{\partial\eta}$$

Ra_m represents Rayleigh-Darcy number which is defined as: $Ra_m = Ra.Da$

The boundary conditions are expressed as following:

Hot inner wall with high concentration ($\eta=\eta_i$=cst):

$$V_\eta^+ = V_\theta^+ = \frac{\partial\psi^+}{\partial\eta} = \frac{\partial\psi^+}{\partial\theta} = 0\ ,\ T_1^+ = 1,\ C_1^+ = 1$$

Cold outer wall with low concentration ($\eta=\eta_e$=cst):

$$V_\eta^+ = V_\theta^+ = \frac{\partial\psi^+}{\partial\eta} = \frac{\partial\psi^+}{\partial\theta} = 0\ ,\ T_2^+ = 0,\ C_2^+ = 0$$

IV. Numerical Method

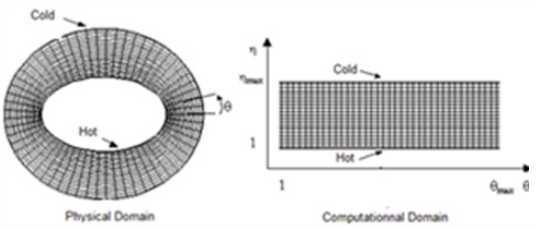

Fig. 2. Physical and computational domain

Fig. 2 shows the physical and computational domain, to solve (11), (12) and (13) with the associated boundary conditions; we consider a numerical solution by the finite volumes method, exposed by [14]. The power law scheme was used for the discretization. To solve (14), we consider a numerical solution by the centered differences method. The iterative method used for the numerical solution of algebraic system of equations is the Gauss-Seidel with an under-relaxation process. Once the temperature and concentration distributions are available, the local Nusselt and Sherwood numbers in the physical domain are defined as:

$$Nu = -\frac{1}{h}\frac{\partial T^+}{\partial\eta}\bigg|_{\eta=cst} \tag{15}$$

$$Sh = -\frac{1}{h}\frac{\partial C^+}{\partial\eta}\bigg|_{\eta=cst} \tag{16}$$

V. Results And Discussion

Our objective is to analyze the effect of low Rayleigh-Darcy number and Buoyancy ratio for the cooperative mode on the flow and the heat and mass transfer. For this reason, we presented streamlines, isotherms and concentration contours for different values of Rayleigh-Darcy number for the case when the buoyancy ratio is equal to zero *N*=0 and for a determined value of Rayleigh-Darcy number Ra_m=50, we presented streamlines, isotherms and concentration contours for different value of buoyancy ratio. The Nusselt and Sherwood numbers were presented for different values of Ra_m and N. The above results were carried out for the case of the air with a Lewis number Le=0.1 when the inclination is α=0°.

A. Influence of Rayleigh-Darcy number (Ra_m)

We consider an annular spaces characterized by the eccentricity of the internal and the external elliptic cylinder respectively given by e1=0.9 and e2=0.5 with the inclination chosen for the calculation is α=0°.

We used different values of Rayleigh-Darcy number from Ra_m=1 to Ra_m=50 for the case when only the thermal gradients are at the origin of the flow, this case is corresponding to a buoyancy number equal to zero (*N*=0).

Fig. 3 to fig. 6 represent the streamlines, isotherms and concentration contours for different values of Rayleigh-Darcy number when *N*=0, Le=0.1 and the inclination α =0°. We note that these contours are symmetrical about the median fictitious vertical plane. The isotherms in fig. 3 and fig. 4 corresponding to Ra_m =1 and Ra_m=10 are parallel and concentric closed curves which coincide perfectly with the walls profile, in this case the temperature distribution is simply decreasing from the hot wall to the cold wall. The concentration contours on the same figure illustrate a similar behavior as isotherms and they correspond perfectly to the walls, the mass distribution is simply decreasing from the high concentration wall to the low concentration wall.

The streamlines of the same figure show that the flow is organized in two main cells that rotate very slowly in opposite directions. This is due to upward movement of the fluid particles which heat up along the hot wall under the

ISBN: 978-988-19253-5-0
ISSN: 2078-0958 (Print); ISSN: 2078-0966 (Online)

buoyancy effect related to temperature gradients only and the downward movements of the fluid particles which cool along the cold wall under the gravity, values of the stream function are very low in this case due to very low Rayleigh-Darcy number. The concentrations variation doesn't have any contribution in the generation of the flow for the case of N=0; the heat and mass transfer takes mainly by conduction and diffusion modes respectively at the heated wall with high concentration, although the velocity fields are nonzero.

Fig. 5 corresponding to Ra_m=30 show that the isotherms are modified, the temperature distribution decreases from the hot wall to the cold wall and the deformation direction of the isotherms is conforming to the direction of streamlines rotation. Values of streams function are increased which means that the convection is present with the increase of the Rayleigh-Darcy number value. The concentration distribution remains with a similar behavior; the contours continue having parallel and concentric closed curves which coincide perfectly with the walls profile.

Fig. 6 for Ra_m=50 illustrates that the increase of Rayleigh-Darcy number reflects a significant intensification of natural convection induced by a thermal-buoyancy effect and shows that the flow remains organized in two main cells rotating in opposite directions but with a higher velocity, the streamlines from both cells tend to became adjacent which reduce the gap between the cells in the upper annulus space. Isotherms in fig. 6 show that the fluid is almost motionless in the bottom of the annular space, in the other hand; isotherms deform into the area where there is presence of two counter-rotating vortices in the upper space. This configuration illustrates a transition in the heat transfer from the pure conduction in the whole space to a convective mode in the upper space. The heat transfer remains dominated by the conduction mode in the lower space. The concentration distribution remains with a similar behavior that corresponds to a mass transfer conducted by a pure diffusion mode.

B. The effect of Rayleigh-Darcy number on local Nusselt and Sherwood numbers

In fig. 7 we illustrated the variation of local Nusselt number on the inner wall of the elliptical cylinder; this variation allows us to note that with the increase of Rayleigh-Darcy number, the value of local Nusselt number increases, which is obvious. For the Nusselt variation the same figure shows for Ra_m=50, an existence of two minimums and two maximums corresponding to a counter-rotating cells.

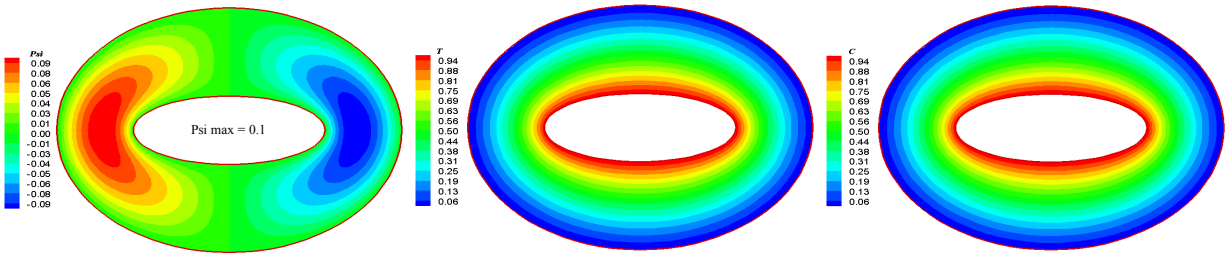

Fig. 3. Streamlines, isotherms and concentration contours for Ra_m=1, Le=0.1 and N=0

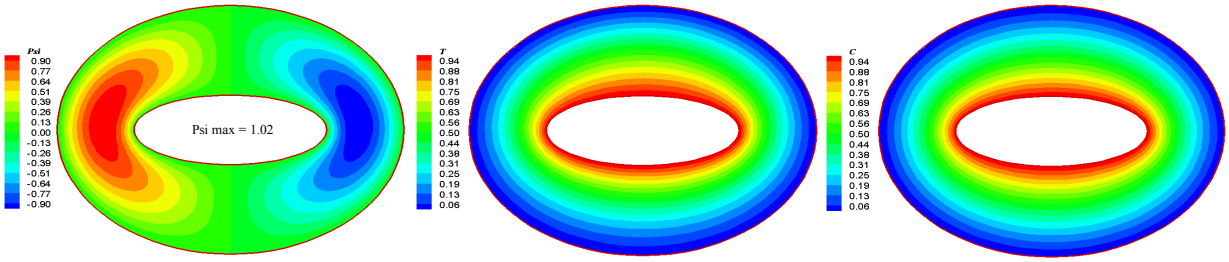

Fig. 4. Streamlines, isotherms and concentration contours for Ra_m=10, Le=0.1 and N=0

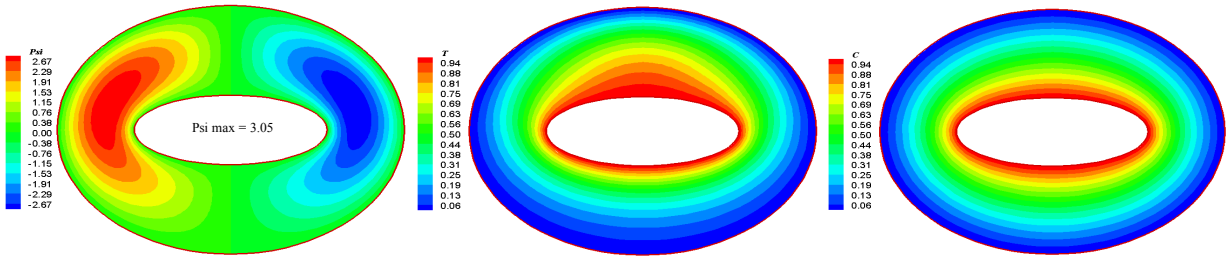

Fig. 5. Streamlines, isotherms and concentration contours for Ra_m=30, Le=0.1 and N=0

ISBN: 978-988-19253-5-0
ISSN: 2078-0958 (Print); ISSN: 2078-0966 (Online)

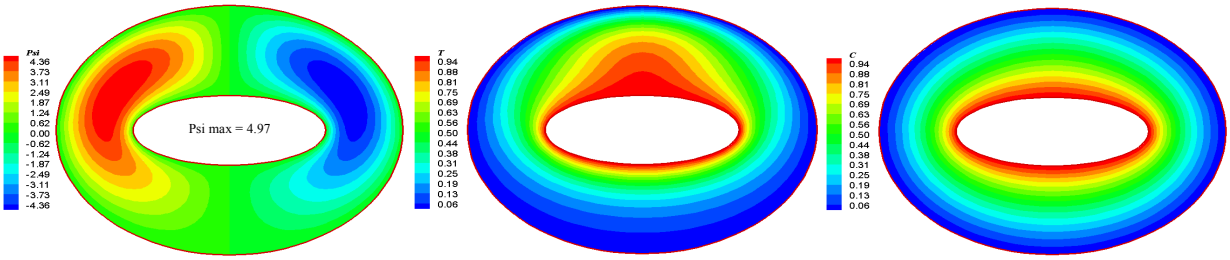

Fig. 6. Streamlines, isotherms and concentration contours for Ra_m=50, Le=0.1 and *N*=0.

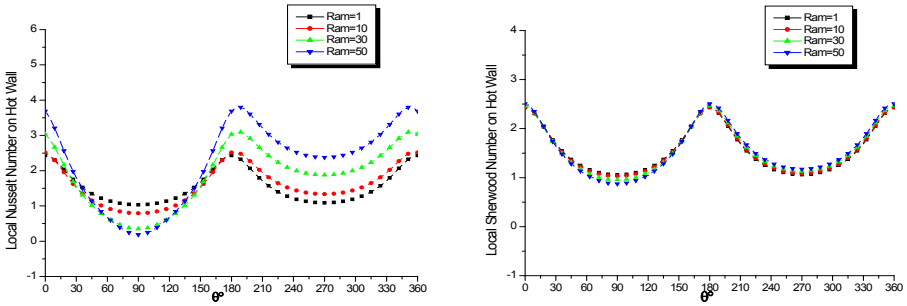

Fig. 7. Variation of local Nusselt and Sherwood numbers on the hot wall for *N*=0.

These cells are pushing away the fluid from the hot wall in the case of a minimum, and bringing the fluid to the wall in the case of a maximum. In the other hand, the local Sherwood number which interprets the mass transfer for the same case of *N*=0, has a same profile with increasing the Rayleigh-Darcy number for this range where the local Sherwood is not sensitive within this range of low Rayleigh-Darcy number values.

C. Influence of the Buoyancy ratio (N)

We consider the same annular spaces characterized by the eccentricity of the internal and the external elliptic cylinder respectively given by e1=0.9 and e2=0.5 with the inclination chosen for the calculation is α=0°. We use different values of the Buoyancy ratio *N*=1, *N*=5, *N*=10 and *N*=50 for the case when the Rayleigh-Darcy number Ra_m=50 and Le=0.1.

Fig. 8 to fig. 11 represent the streamlines, isotherms and concentration contours for different values of Buoyancy ratio. With increasing the buoyancy ratio *N*>0 and for the case of *N*=1 as shown in fig. 8 the flow remains organized in two main cells that rotate in opposite directions and it is clear that the solutal buoyancy force which increases with the buoyancy ratio is cooperating with the thermal buoyancy and they drive the fluid in the same direction to form a cooperator flow, where the stream function levels have a significant increase with increasing in buoyancy ratio due to aiding effect of thermal and solutal buoyancies. The isotherms contours are maintained on the same previous behavior when the only thermal buoyancy was acting, but the gradients are stronger and increase directly with the increasing the buoyancy ratio. A slight change arisen in the concentration contours which are not perfectly coinciding with the walls shape, this change announce that a mass transfer is generated by the solutal buoyancy and contributes in the flow structure.

Fig. 9 and fig. 10 corresponding to *N*=5 and *N*=10 show that the concentration contours present an intensification due the increase of the buoyancy ratio; the solutal buoyancy is contributing and gaining more implication in the flow. The concentration contours tend to have a shape of a dome in the upper space. The isotherms are modified from a dome shaped in the case of *N*=0 for the same value of Rayleigh-Darcy number to a mushroom shaped due to the increase in the buoyancy ratio that gives a preponderant effect to the solutal buoyancy for the flow structure.

The temperature distribution is gaining more regions in the lower annular space due to the high temperature gradients induced by the aiding effect of solutal and thermal buoyancies. Streamlines in these figures show that the flow remains organized in two main cells, but with increasing buoyancy ratio these two cells tend to decline towards the right and left sides of the annular space, the stream function levels have a significant increase with increasing in buoyancy ratio due to the aiding effect.

Fig. 11 represents streamlines, isotherms and concentration contours for *N*=50, the solutal distribution is intensified and the concentration gradients have a significant increase with the increase of buoyancy ratio, the mass transfer is almost gaining all the half upper space. In the lower space, the concentration contours tend to become very close to each other near the lower hot wall which is a result of the preponderant convective role in the mass transfer.

The isotherms have a significant change with a cone shaped curves, the convective heat transfer is gaining more space due the intensification of the flow which is dominated by a high solutal buoyancy forces. The streamlines shown in fig. 11 have completely transformed from smooth curved cells to narrow cells that rotate in opposite directions but

ISBN: 978-988-19253-5-0
ISSN: 2078-0958 (Print); ISSN: 2078-0966 (Online)

with a very high velocity, both cells decline towards the right and the left side in the annular space under the high velocity of streams function, this configuration demonstrates that the heat and mass transfer is dominated by the solutal forces under a convective mode.

D. The effect of Buoyancy ratio on local Nusselt and Sherwood numbers

In fig. 12 we illustrated the variation of the local Nusselt and Sherwood numbers on the inner wall of the elliptical cylinder. The variation of the local Nusselt number allows us to note that with the increase in the buoyancy ratio, its value increases due to the increase in the flow that gives a better heat transfer under a convective mode.

The Nusselt variation in fig. 12 shows for Ra_m=50, a presence of three maximums in the lower side of the enclosure (190°<θ<330°), two of them are corresponding to the maximum velocities of both counter-rotating cells that bringing the fluid to the cold region from both sides where the heat exchange is active. The third maximum corresponding to the middle point in the lower hot wall which is expressing an additional intensive conductive heat exchange made in a very thin boundary layer where the motionless fluid is directly in contact with the hot wall.

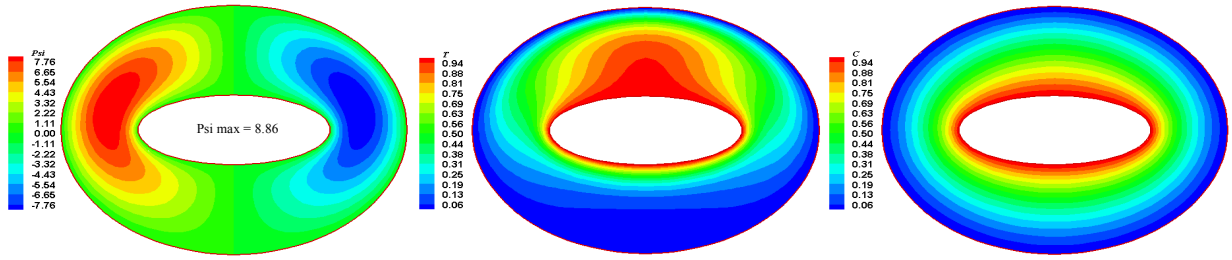

Fig. 8. Streamlines, isotherms and concentration contours for Ra_m=50, Le=0.1 and *N*=1

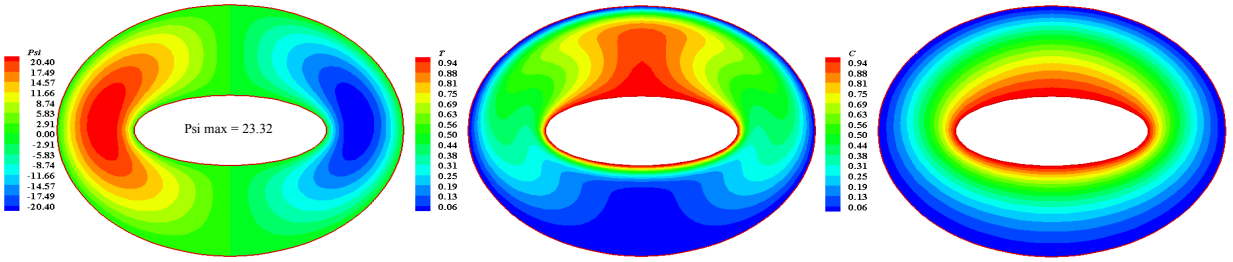

Fig. 9. Streamlines, isotherms and concentration contours for Ra_m=50, Le=0.1 and *N*=5

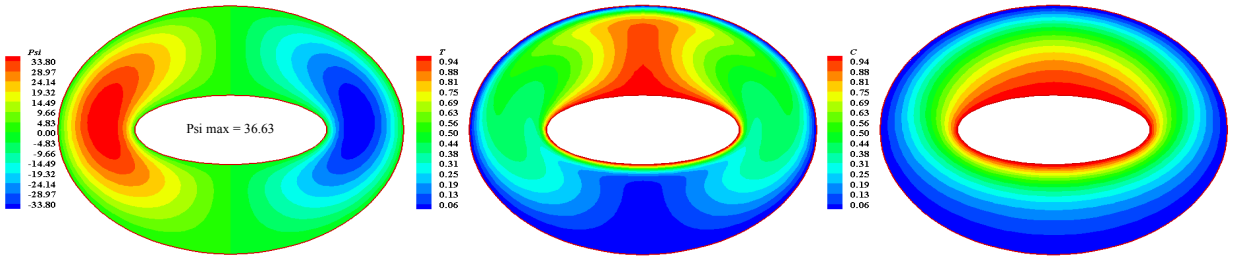

Fig. 10. Streamlines, isotherms and concentration contours for Ra_m=50, Le=0.1 and *N*=10

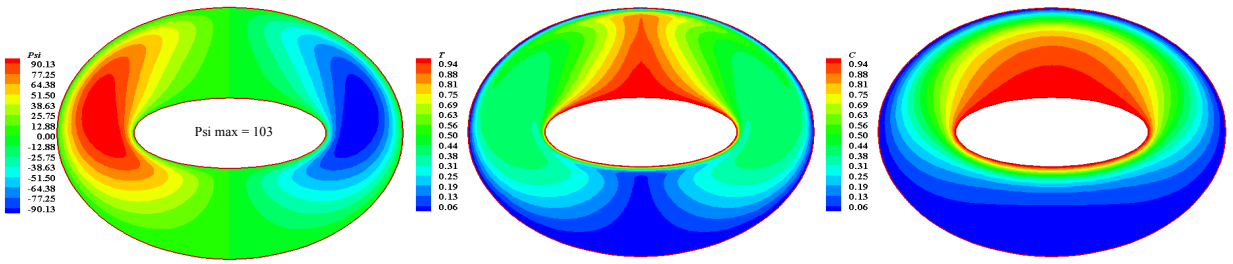

Fig. 11. Streamlines, isotherms and concentration contours for Ra_m=50, Le=0.1 and *N*=50

ISBN: 978-988-19253-5-0
ISSN: 2078-0958 (Print); ISSN: 2078-0966 (Online)

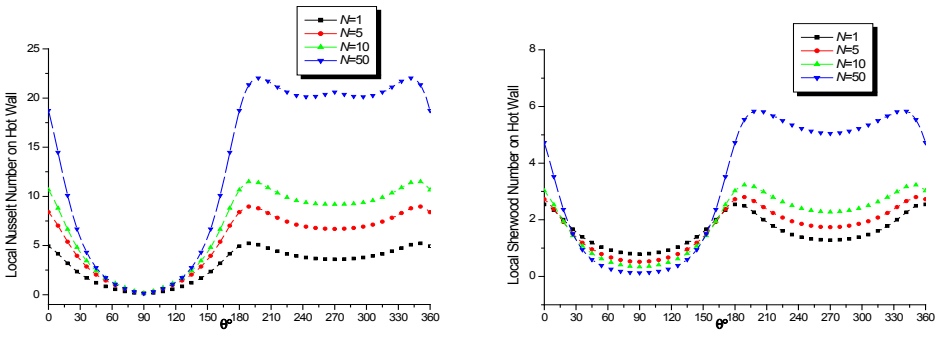

Fig. 12. Variation of local Nusselt and Sherwood numbers on the hot wall for Ra_m=50

The local Sherwood number illustrates a significant increase with increasing the buoyancy ratio, which is obvious because the solutal buoyancy forces increase. However, the mass transfer remains moderate with a qualitative comparison to the heat transfer due to the low value of Lewis number.

VI. Conclusion

The thermosolutal natural convection in a porous elliptical annulus saturated by a Newtonian fluid was studied using a numerical method using the method of finite volumes, the vorticity-streamline formulation, makes it possible to find a good agreement with the literature of bidimensional thermal natural convection for a laminar and permanent flow in an annular space filled with fluid-saturated porous media located between two confocal elliptic cylinders.

We examined, in particular, the influence of low Rayleigh-Darcy number range for the case when only the thermal buoyancy is at the origin of the fluid flow and the effects of aiding buoyancies using different values of buoyancy ratio. Different structures of bicellular convection take place according to the value of the Rayleigh-Darcy number, when the solutal buoyancy ratio is equal to zero, only the thermal forces are generating the flow.

The heat transfer is transiting form a conductive mode to a convective mode with increasing Rayleigh-Darcy number. In the other hand, the mass transfer remains dominated by a diffusive mode when only the thermal buoyancy is generating the flow for a low values of Rayleigh-Darcy number. The heat and mass transfer are both involved in the flow structure when the values of buoyancy ratio are nonzero and positive. The solutal buoyancy forces which increase with the buoyancy ratio are cooperating with the thermal buoyancy forces and they drive the fluid in the same direction to form a cooperator flow, where the aiding effect is observed by an intensification of the heat and mass transfer with a significant evolution in the flow structure.

References

[1] M. Sankar, Youngyong Park, J.M. Lopez, Younghae Do: Numerical study of natural convection in a vertical porous annulus with discrete heating, Int. J. Heat and Mass Transfer (2011), 54, pp. 1493-1505.

[2] F.M. Mahfouz “Buoyancy driven flow within an inclined elliptic enclosure,” International Journal of Thermal Sciences, 50 (2011), pp. 1887-1899

[3] Khalil Khanafer, Abdalla Al-Amiri, Ioan Pop “Numerical analysis of natural convection heat transfer in a horizontal annulus partially filled with a fluid-saturated porous substrate,” Int. J. Heat and Mass Transfer (2008), 51, pp.1613-1627.

[4] Kumari, M. and Nath, G. “Unsteady natural convection from a horizontal annulus filled with a porous medium, Int. J. Heat and Mass Transfer (2008),” 51, pp. 5001-5007.

[5] Yong Shi, T.S. Zhao, Z.L. Guo “Finite difference-based lattice Boltzmann simulation of natural convection heat transfer in a horizontal concentric annulus,” Computers & Fluids 35 (2006), pp. 1–15.

[6] Edimilson J. Braga and Marcelo J.S. de Lemos “Simulation of turbulent natural convection in a porous cylindrical annulus using a macroscopic two-equation model,” International Journal of Heat and Mass Transfer 49 (2006), pp. 4340–4351

[7] Leong, J.C. and Lai, F.C. “Natural convection in a concentric annulus with a porous sleeve,” Int. J. Heat and Mass Transfer (2006), 49, pp. 3016-3027.

[8] M. Djezzar, A. Chaker and M. Daguenet “Numerical Study of bidimensional steady natural convection in a space annulus between two elliptic confocal ducts, influence of the eccentricity,” Rev. Energy. Ren. Vol.8 (2005), pp. 63-72.

[9] Y.D. Zhu, C. Shu, J. Qiu, J. Tani “Numerical simulation of natural convection between two elliptical cylinders using DQ method,” International Journal of Heat and Mass Transfer 47 (2004), pp. 797–808

[10] Wassim Chmaissem, Seung JikSuh, Michel Daguenet “Numerical study of the Boussinesq model of natural convection in an annular space: having a horizontal axis bounded by circular and elliptical isothermal cylinders,” Applied Thermal Engineering 22 (2002), pp. 1013–1025

[11] J.P.B. Mota, I.A.A.C. Esteves, C.A.M. Portugal, J.M.S.S. Esperanca, E. Saatdjian “Natural convection heat transfer in horizontal eccentric elliptic annuli containing saturated porous media,” Int. J. Heat and Mass Transfer (2000), 43, pp. 4367-4379.

[12] Charrier-Mojtabi, M. C. “Numerical simulation of two- and three-dimensional free convection flows in a horizontal porous annulus using a pressure and temperature formulation,” Int. J. Heat and Mass Transfer (1997), 40, pp. 1521-1533.

[13] M. M. Elshamy and M. N. Ozisik “Correlation for laminar natural convection between confocal horizontal elliptical cylinders,” Numerical Heat Transfer, Part A, vol.18 (1990), pp.95-112.

[14] Patankar, S.V. (1980) “Numerical heat transfer and fluid flow,” Hemisphere, Washington D.C.

ISBN: 978-988-19253-5-0
ISSN: 2078-0958 (Print); ISSN: 2078-0966 (Online)